1.1 W continuous-wave, narrow spectral width (<1 Å) emission from broad-stripe, distributed-feedback diode lasers ($\lambda = 0.893\ \mu m$)

T. Earles,[a] L. J. Mawst, and D. Botez
Reed Center for Photonics, ECE Department, University of Wisconsin–Madison, Madison, Wisconsin 53706

(Received 10 June 1998; accepted for publication 6 August 1998)

By etching a distributed-feedback grating directly into the Al-free optical confinement region of a 100 μm stripe InGaAs/InGaP/GaAs diode laser, 1.1 W cw front-facet output power has been obtained at 0.893 μm with a spectral full width at half maximum of 0.9 Å. These devices have 1 mm long cavities and shallow gratings with a coupling coefficient, $\kappa \sim 7\ cm^{-1}$. The combination of long device length and low grating coupling results in both efficient operation as well as a longitudinally uniform field profile. As a result, all excited lateral modes oscillate at the same longitudinal cavity resonance to high power levels. Using shallow gratings etched in an InGaP upper confinement layer permits the growth of a high-quality cladding layer over the grating surface yielding excellent device performance. Facet-coated (5%/95%) devices demonstrate external differential quantum efficiencies of 51% and peak wallplug efficiencies of 32% at 1.1 W cw output power. © *1998 American Institute of Physics.* [S0003-6951(98)00441-0]

High-power, narrow spectral width semiconductor lasers have application potential for magnetic resonance imaging (MRI) using laser-polarized noble gases, gas spectroscopy, and as low chirp pump sources for solid-state lasers. Of particular interest for MRI are 0.894 μm diode lasers that may be used for polarizing Cs in a process to generate spin-polarized Xe gas.[1] For this application, watt-range cw powers and narrow spectral width, <2 Å full width half maximum (FWHM), are required to obtain efficient polarization of the Cs atoms without the need of excessive gas temperatures or pressures. These objectives have been attained by using broad-stripe distributed feedback lasers with shallow gratings made in an Al-free optical confinement region.

Conventional broad-stripe Fabry–Perot diode lasers used for obtaining high powers generally have a spectral full width at half maximum of ~20 Å or more at high drive levels[2] and broaden further under quasi-cw operation.[3] In order to narrow the spectrum of diode lasers, frequency selective feedback from index-coupled gratings may be used for passive wavelength control in the form of distributed feedback (DFB) or distributed Bragg reflectors (DBR). DFB lasers that use the GaAs/AlGaAs material system are difficult to make because of the high reactivity of Al to oxygen.[4] Large performance penalties result from the oxidation that occurs during fabrication of AlGaAs gratings. To alleviate the problem, devices with the grating outside the active region (i.e., DBR lasers) have been employed. Single-mode powers as high as 278 mW have been obtained from narrow stripe (4 μm) DBR lasers.[5] However, DBR lasers show severe mode hopping at high power levels due to thermally induced changes in the refractive index of the active region.[6] As a consequence, stable single-mode operation only occurs over small power intervals separated by spectrally noisy transition regions. In order to improve the interface quality for DFB lasers on GaAs substrates, gratings have been placed on InGaP cladding layers below the active region of the laser structures.[7,8] Sagawa *et al.*[7] used a structure with InGaAsP confinement layers, but the quaternary regrowth over the grating was apparently of poor quality yielding relatively poor device performance. Sin and Horikawa[8] described a structure using GaAs confinement layers and InGaP cladding layers. The binary alloy produces a higher quality regrowth, but the low barrier heights of the structure results in poor carrier confinement to the quantum well. In turn, this gives rise to carrier leakage out of the quantum wells.

Here, we present results from 100 μm stripe DFB lasers operating at a wavelength of 0.893 μm that demonstrate high power, narrow spectral width, and excellent performance. These double quantum well, separate confinement heterostructure (DQW-SCH) lasers use a broad, Al-free waveguide with a DFB grating etched in its upper surface. The lasers are fabricated in a two-growth process. The absence of exposed Al-containing compounds during the fabrication of the grating provides for good regrowth quality yielding low interface loss. This promotes high external differential quantum efficiencies of 51% and high peak wallplug efficiencies of 32% at 1.1 W. The spectra of these devices driven at high powers have a half width of 0.9 Å at 1.1 W cw, and 1.2 Å at 1 W pulsed (5 μs, 2 kHz). Subthreshold spectra analysis reveals a relatively small coupling κL value of 0.7, which provides for the efficient operation of the lasers.

A schematic of the DFB laser structure is shown in Fig. 1. The SCH consists of two $In_{0.03}Ga_{0.97}As$ quantum wells within an $In_{0.47}Ga_{0.53}P$ optical confinement region that is surrounded by $In_{0.5}(Ga_{0.5}Al_{0.5})_{0.5}P$ cladding layers. The 55 Å quantum wells are bounded by 200 Å InGaAsP ($E_g = 1.62$ eV) transition layers to improve the interface quality. The optical confinement region thickness of 6500 Å is below the cutoff thickness for the second-order transverse mode. This insures lasing of the fundamental transverse mode, since the first-order mode is suppressed by its poor optical confinement factor. The large band gap of the $In_{0.5}(Ga_{0.5}Al_{0.5})_{0.5}P$ cladding layers insures good carrier con-

[a]Electronic mail: earles@cae.wisc.edu

 © 1998 American Institute of Physics
Downloaded 21 Dec 2006 to 128.104.30.229. Redistribution subject to AIP license or copyright, see http://apl.aip.org/apl/copyright.jsp

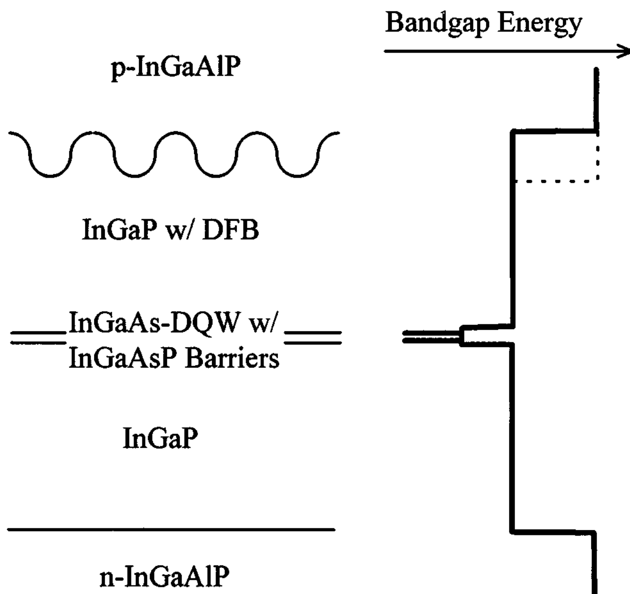

FIG. 1. Schematic cross section of DFB 0.893 μm emitting laser structure. The active region consists of two 55 Å wide $In_{0.03}Ga_{0.97}As$ quantum wells surrounded by 200 Å thick InGaAsP ($E_g = 1.62$ eV) barriers and 0.3 μm thick InGaP confinement layers. The grating has a period of 2740 Å and a depth of ~500 Å.

finement for the structure,[9] resulting in higher internal efficiencies and less temperature sensitivity than would be obtained from an entirely Al-free structure.

The broad-stripe DFB lasers are fabricated in a two-step metal–organic chemical vapor deposition (MOCVD) growth process. The laser base (lower clad and active region) is grown at a temperature of 700 °C on a (100) n^+-GaAs substrate. A holographically patterned second-order grating ($\Lambda = 2740$ Å) is wet etched directly into the InGaP confinement layer over the active region. The best results have been from 500 Å deep gratings anisotropically etched along the ⟨011⟩, ''dovetail,'' direction. The overgrowth is performed under the same growth conditions as the base. Surface mass transport that occurs during regrowth yields a nearly sinusoidal

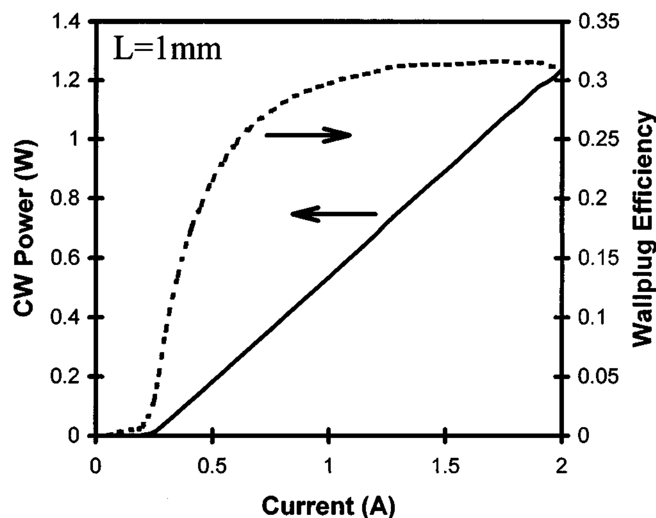

FIG. 2. Cw light current and wallplug efficiency η_p, characteristics for a 100 μm×1 mm contact area, 5%/95% facet-coated DFB laser ($\lambda = 0.893$ μm) at 10 °C heatsink temperature. The differential quantum efficiency is 51% and the η_p reaches a maximum of 32% at 1.1 W.

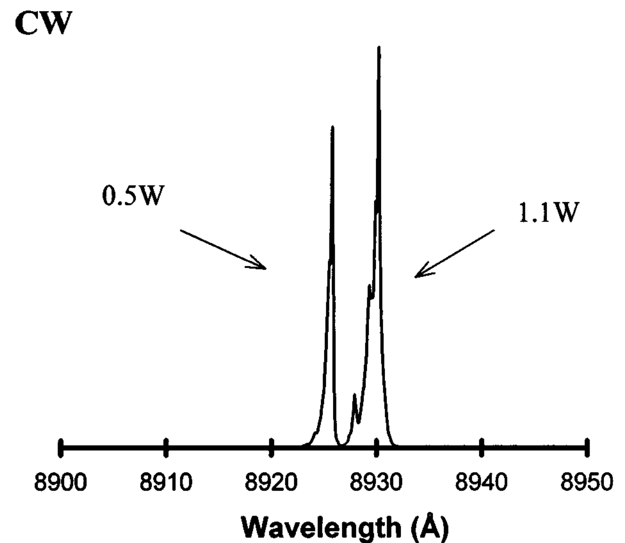

FIG. 3. High-power cw spectra for 100 μm stripe DFB laser operation at 10 °C heatsink temperature. The spectra have a temperature dependence of 0.6 Å/°C.

corrugation. Because InGaP is much less prone to oxidation than Al-containing compounds, no special procedures are necessary for regrowth. Thus, the InGaAlP cladding layer is simply grown over the grating followed by a p^+-GaAs cap layer for good ohmic contact. An oxide-defined 100 μm stripe laser structure is processed from this material, and bars are cleaved and facet coated to produce 1 mm long lasers with 5%/95% facet reflectivities. This grating fabrication technique is directly applicable to lasers at many other wavelengths such as 0.808 μm emitting Al-free active region lasers for pumping Nd–YAG lasers.

The cw P–I curve for a 1 mm long, 100 μm wide DFB laser at 10 °C is shown in Fig. 2. The threshold current density J_{th} is 240 A/cm^2; the differential quantum efficiency η_d, is 51%; and the peak wallplug efficiency η_p, reaches a maximum value of 32% at 1.1 W (7.3× threshold). By comparison, Fabry–Perot devices made without gratings, but with the same structure and dimensions have at 20 °C a J_{th} of 225 A/cm^2 and η_d of 62% with characteristic temperatures for threshold current density and external differential quantum efficiency of $T_0 = 200$ K and $T_1 = 480$ K, respectively.

Spectral measurements were performed on the broad-area DFB lasers with a 1.25 m spectrometer and a photomultiplier tube. The spectrum is predominantly single frequency near threshold with a temperature dependence of 0.6 Å/°C and maintains a narrow linewidth up to 1 W output power (Fig. 3). The FWHM for the cw spectrum at 0.53 W is 0.5 Å FWHM, and at 1.1 W, if we approximate a width based upon the envelope of the peaks, the spectrum broadens to about 0.9 Å FWHM. Under pulsed-current conditions the spectrum is broader than the cw spectrum, which can be attributed to thermal and carrier density transients (chirp). The spectra of the lasers measured with 5 μs pulses at a frequency of 2 kHz yield widths of 0.9 and 1.2 Å FWHM at 0.5 and 1.0 W, respectively. In contrast, the near-threshold spectra of the Fabry–Perot lasers with the same structure have a width of over 10 Å FWHM, and reach 20 Å FWHM at 1 W cw.

Parameter extraction has been performed on these lasers by fitting the measured amplified spontaneous emission

Downloaded 21 Dec 2006 to 128.104.30.229. Redistribution subject to AIP license or copyright, see http://apl.aip.org/apl/copyright.jsp

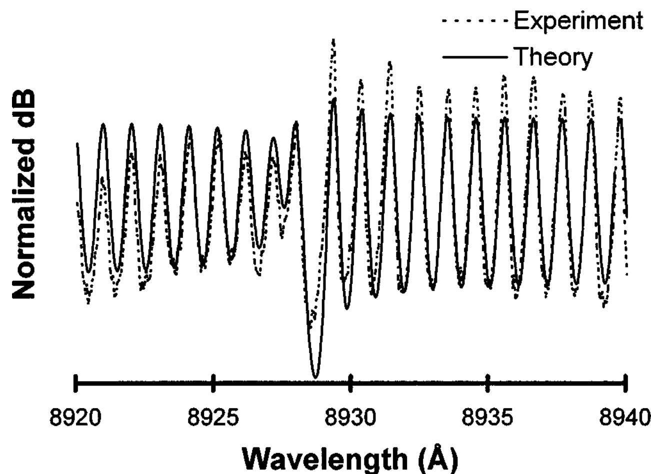

FIG. 4. Comparison of theoretical and experimental amplified spontaneous emission spectra. The modeled spectrum has a κL value of 0.7.

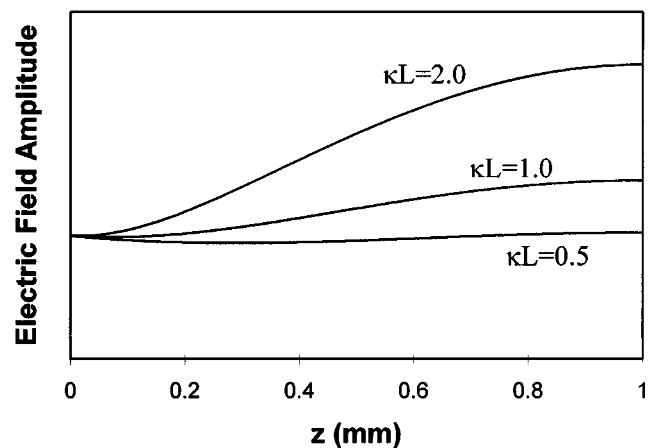

FIG. 5. Calculated longitudinal field profile of an asymmetrically coated DFB laser for different values of κL. The endpoints, at $z=0$ and $z=1$ nm, correspond to 5% and 95% facet coated mirrors, respectively.

(ASE) spectrum to a simple model as described by Schatz *et al.*[10] Figure 4 shows a measured subthreshold spectrum and the modeled ASE. From the fit, we have determined approximate values for the coupling coefficient, $\kappa \sim 7\ \mathrm{cm}^{-1}$, and the effective mirror loss for the DFB, $\alpha_{\mathrm{DFB}} \sim 6\ \mathrm{cm}^{-1}$. The fitted coupling coefficient is slightly lower than the calculated value of 9.5 cm^{-1} for a perfectly sinusoidal grating using perturbation theory.[11] The low coupling ($\kappa L \sim 0.7$) provides a more uniform field profile along the cavity than devices with highly coupled gratings. Calculated field profiles for DFB lasers with asymmetrically coated facets (5%/95%) are shown in Fig. 5. The calculations, based on the general solutions to the coupled-mode equations,[12] assume no phase shifts at the facets. It can be seen that κL values between 0.5 and 1 should provide relatively uniform longitudinal field profiles. This suppresses the multiple-longitudinal-mode operation caused by longitudinal gain spatial hole burning that occurs in more highly coupled devices. Thus, the narrow spectral width is predominantly due to simultaneous oscillation of lateral spatial modes that share the same longitudinal mode number. Furthermore, a lower coupling will increase the facet loss of the DFB producing a higher differential quantum efficiency.[13]

The internal loss coefficient α_i, of the lasers can be determined by detuning the gain spectrum of the lasers such that they operate in Fabry–Perot modes. The measured differential quantum efficiencies for one device is $\eta_d^{\mathrm{DFB}} = 51\%$ and $\eta_d^{\mathrm{FP}} = 67\%$. Using the calculated mirror loss α_m, for the Fabry–Perot laser of 15 cm^{-1} and assuming a 100% internal quantum efficiency η_i, the α_i was determined to be about 7 cm^{-1}. Consequently, the facet loss of the DFB, α_{DFB}, must be approximately 7 cm^{-1}, which is in good agreement with the value obtained from the ASE parameter fitting. These results are of particular interest because the average α_i of devices without gratings was measured to be 6.6 cm^{-1}, implying that the shallow gratings contribute very little to the internal loss of the devices.

For applications where high power and narrow spectral width are necessary, we have demonstrated that a broad-area laser with an Al-free broad-waveguide structure can easily be turned into a high power (1 W), narrow spectrum (1 Å FWHM) source by placing a DFB grating directly on the optical confinement region. In addition, the introduction of the gratings did not seriously affect the performance of the lasers.

Special thanks to Jeff Morris of LDX Optronics for lending the authors his packaging expertise, and Dan Christensen and Dave Jones of the Wisconsin Center of Applied Microelectronics for their technical assistance. This work was supported by the National Science Foundation, Grant No. BES-9612244.

[1] M. S. Albert, G. D. Cates, B. Driehuys, W. Happer, B. Saam, C. S. Springer, Jr., and A. Wishnia, Nature (London) **370**, 199 (1994).
[2] L. J. Mawst, A. Bhattacharya, J. Lopez, D. Botez, D. Z. Garbuzov, L. DeMarco, J. C. Connolly, M. Jansen, F. Fang, and R. F. Nabiev, Appl. Phys. Lett. **69**, 1532 (1996).
[3] A. Al-Muhanna, L. J. Mawst, D. Botez, D. Z. Garbuzov, R. U. Martinelli, and J. C. Connolly, Appl. Phys. Lett. **71**, 1142 (1997).
[4] P. K. York, J. C. Connolly, N. A. Highes, T. J. Zamerowski, J. H. Abeles, J. B. Kirk, J. T. McGinn, and K. B. Murphy, J. Cryst. Growth **124**, 709 (1992).
[5] J. S. Major, Jr. and D. F. Welch, Electron. Lett. **29**, 2121 (1993).
[6] J. S. Major, Jr., S. O'Brien, V. Gulgazov, D. F. Welch, and R. J. Lang, Electron. Lett. **30**, 496 (1994).
[7] M. Sagawa, K. Hiramoto, T. Tsuchiya, and S. Tsuji, Electron. Lett. **28**, 2336 (1992).
[8] Y. K. Sin and H. Horikawa, Electron. Lett. **29**, 920 (1993).
[9] J. K. Wade, L. J. Mawst, D. Botez, R. F. Nabiev, M. Jansen, and J. A. Morris, Appl. Phys. Lett. **72**, 4 (1998).
[10] R. Schatz, E. Berglind, and L. Gillner, IEEE Photonics Technol. Lett. **6**, 1182 (1994).
[11] W. Streifer, S. R. Scifres, and R. D. Burnham, IEEE J. Quantum Electron. **QE-11**, 867 (1975).
[12] J. Buus, *Single Frequency Semiconductor Lasers* (SPIE Optical Engineering, Bellingham, WA, 1991), p. 37.
[13] T. R. Chen, W. Hsin, and N. Bar-Chaim, Appl. Phys. Lett. **72**, 1269 (1998).

Downloaded 21 Dec 2006 to 128.104.30.229. Redistribution subject to AIP license or copyright, see http://apl.aip.org/apl/copyright.jsp